

unVEil the darknesS of The gAlactic buLgE (VESTALE)

G. Bono,^{1,2} M. Dall’Ora,³ M. Fabrizio,^{2,4} J. Crestani,^{1,2,5} V.F. Braga,^{6,7} G. Fiorentino,⁸ G. Altavilla,^{2,4} M.T. Botticella,³ A. Calamida,⁹ M. Castellani,² M. Catelan,¹⁰ B. Chaboyer,¹¹ C. Chiappini,³⁷ W. Clarkson,¹² R. Contreras Ramos,^{6,10} O. Creevey,¹³ R. da Silva,^{2,4} V. Debattista,¹⁴ S. Degl’Innocenti,^{15,16} I. Ferraro,² C.K. Gilligan,¹¹ O. Gonzalez,¹⁷ K. Hambleton,⁴⁰ G. Iannicola,² L. Inno,¹⁸ A. Kunder,¹⁹ B. Lemasle,²⁰ L. Magrini,¹⁸ D. Magurno,^{1,2} M. Marconi,³ M. Marengo,²¹ S. Marinoni,^{2,4} P.M. Marrese,^{2,4} C.E. Martínez-Vazquez,²² N. Matsunaga,²³ M. Monelli,^{24,25} P.G. Prada Moroni,^{15,16} I. Musella,³ M.G. Navarro,^{26,7,6} J. Neeley,²⁷ M. Nonino,²⁸ A. Pietrinferni,²⁹ L. Pulone,² M.R. Rich,³⁸ V. Ripepi,³ G. Sacco,¹⁸ A. Saha,²² M. Salaris,³⁰ C. Sneden,³¹ P.B. Stetson,^{32,33} R.A. Street,³⁹ R. Szabo,³⁴ M. Tantalò,¹ E. Tognelli,^{35,15,16} M. Torelli,² E. Valenti,³⁶ A.R. Walker,²² and M. Zoccali^{10,6},

with the support of the LSST Transient and Variable Stars Collaboration.

November 29, 2018

Abstract

The main aim of this experiment is to provide a complete census of old ($t \geq 10$ Gyr, RR Lyrae, type II Cepheids, red horizontal branch), intermediate age (red clump, Miras) and young (classical Cepheids) stellar tracers across the Galactic Bulge. To fully exploit the unique photometric quality of LSST images, we plan to perform a *Shallow minisurvey* ($ugrizy$, $-20 \lesssim l \lesssim 20$ deg, $-15 \lesssim b \lesssim 10$ deg) and a *Deep minisurvey* (izy , $-20 \lesssim l \lesssim 20$ deg, $-3 \lesssim b \lesssim 3$ deg). The former one is aimed at constraining the 3D structure of the galactic Bulge across the four quadrants, and in particular, the transition between inner and outer Bulge. The u, g, r, i, z, y LSST bands provide fundamental diagnostics to constrain the evolutionary properties of low and intermediate-mass stars when moving from a metal-poor to a metal-rich regime. The deep minisurvey is aimed at tracing RR Lyrae, Red Clump stars, Miras and classical Cepheids in highly reddened regions of the Galactic center. These images will allow us to investigate the role that baryonic mass and dark matter played in the early formation and evolution of the MW.

1 White Paper Information

1. **Science Category:** the basic science theme of this project is the Milky Way Structure and Formation. However, since it is based on variable stars as population tracers and distance indicators, it is also related to the Explore the Changing Sky theme.
2. **Survey Type Category:** mini survey.
3. **Observing Strategy Category:** this is a project aimed at detecting variable stars in the MW Bulge. Therefore, it is an integrated program with science that hinges on the combination of pointing and detailed observing strategy.

4. Author Information

¹Università di Roma Tor Vergata

²INAF–Osservatorio Astronomico di Roma

³INAF–Osservatorio Astronomico di Capodimonte

⁴Space Science Data Center–ASI

⁵Universidade Federal do Rio Grande do Sul

⁶Instituto Milenio de Astrofísica

⁷Universidad Andrés Bello

⁸INAF–OAS Osservatorio di Astrofisica & Scienza dello Spazio di Bologna

⁹Space Telescope Science Institute

¹⁰Pontificia Universidad Católica de Chile

¹¹Dartmouth College

¹²University of Michigan-Dearborn

¹³Université Côte d’Azur

¹⁴University of Central Lancashire

¹⁵Università di Pisa

¹⁶INFN, Sezione di Pisa

¹⁷UK Astronomy Technology Centre, Royal Observatory

¹⁸INAF–Osservatorio Astrofisico di Arcetri

¹⁹Saint Martin’s University

²⁰Zentrum für Astronomie der Universität Heidelberg

²¹Iowa State University

²²National Optical Astronomy Observatory

²³The University of Tokyo

²⁴Instituto de Astrofísica de Canarias

²⁵Universidad de La Laguna

²⁶Università di Roma La Sapienza

²⁷Florida Atlantic University

²⁸INAF–Osservatorio Astronomico di Trieste

²⁹INAF–Osservatorio Astronomico d’Abruzzo

³⁰Liverpool John Moores University

³¹University of Texas

³²Dominion Astrophysical Observatory

³³National Research Council of Canada

³⁴Konkoly Observatory

³⁵INAF–Osservatorio Astronomico di Collurania

³⁶European Southern Observatory

³⁷Leibniz Institut fuer Astrophysik Potsdam - AIP

³⁸Department of Physics & Astronomy, The University of California

³⁹Las Cumbres Observatory

⁴⁰Villanova University, Dept. of Astrophysics and Planetary Science

2 Scientific Motivation

This experiment is aimed at disentangling the stellar content of the Galactic Bulge using variable stars, since they have the advantage to provide individual distance, age, metallicity and reddening estimates. We focus our attention on variables tracing old (RR Lyraes, RRLs; Type II Cepheids, TIICs; $t > 10$ Gyr), intermediate-age (Miras, $t \sim 0.5\text{--}10$ Gyr), and young (Classical Cepheids, CC; $t \sim 10\text{--}300$ Myr) stellar populations (Bono et al. 2015; Matsunaga et al. 2016). The Galactic Bulge, which is mainly old with a younger tail, makes up the 25% of the total MW stellar mass (Valenti et al. 2016). Recent photometric and spectroscopic investigations revealed that the Bulge contains two main components. The old and/or metal-poor one, traced either with RRL or with metal-poor Red Clump (RC) stars, is rounder, rotates slower and has a shallower gradient in radial velocity dispersion. The metal-rich one is traced with RC stars, it is arranged in a bar that flares up into a boxy/peanut structure in its outer region, rotates faster, and has a steeper gradient in radial velocity dispersion (Ness et al. 2012; Rojas-Arriagada et al. 2014; Pietrukowicz et al. 2015; Kunder et al. 2016; Zoccali et al. 2017). Recent spectroscopic surveys mainly based on either giants (BRAVA; Shen et al. 2010) or RC stars (ARGOS; GIBS; Freeman et al. 2013; Zoccali et al. 2014) suggest that Bulge stars undergo cylindrical rotation. On the other hand, BRAVA-RR used RRLs and found much slower rotations, and higher velocity dispersions (Barbuy et al. 2018). Moreover, it is not clear yet whether Bulge RRLs trace either the main Bar or the spheroidal component (Dékány et al. 2013; Pietrukowicz et al. 2015; Kunder et al. 2018).

Why a shallow minisurvey

- *3D Bulge Structure* – We have recently developed a new algorithm to estimate reddening distance and metallicity (REDIME) by using optical/NIR (BVIJHK) bands (Bono et al. 2018). The key advantage of this approach is that we can provide the 3D structure of the Bulge, a 3D reddening map and a homogeneous metallicity distribution of the entire sample of RRLs using "blue" (ugr) and "red" (izy) LSST bands. The zero-point of the metallicity distribution might be affected by the accuracy of the adopted reddening law and of the distance diagnostic. However, we are interested in the differential variation and the accuracy is ~ 0.2 dex. This means new constraints on the occurrence of a metallicity gradient across the Bulge (Hill et al. 2011; Zoccali et al. 2017); the shape of the Bulge in the four quadrants; the real extent and geometry of both inner and long Bar (Hammersley et al. 2000; Athanassoula 2005). We are also interested in estimating the position angle and the inclination of the Bar by using old (RRLs, TIICs), intermediate age (RC, Miras) and young (classical Cepheids) stars to constrain its secular stability (Wegg & Gerhard 2013).

- *Bulge stellar populations* – The current structure of the Bulge mainly relies on RC stars, i.e. old/intermediate age stellar tracers. However, solid theoretical (Salaris et al. 2003) and empirical (Stetson et al. 2011) evidence indicates that RC stars are intermediate-mass, central helium burning stars, while red HB stars are low-mass, central helium burning stars. The difference in visual magnitude, at fixed metal content, is at least of the order of 0.5 magnitude, while the optical colors are, at solar chemical compositions, quite similar (see Fig. 1). The two subpopulations have never been identified in the Bulge due to a mix between

photometric error and differential reddening. Data plotted in Fig. 2 indicate that LSST can trace the variation between the two different sub-populations across the entire Bulge. We also plan to use the equivalent of the C_{UBI} ($[U-B]-[B-I]$) photometric index (Monelli et al. 2016), but for the SDSS bands C_{ugr} ($[u-g]-[g-i]$) to separate old and intermediate-age Bulge stars (Fabrizio et al. 2016). Moreover, the spectral energy distribution ($ugri$ bands) to separate Disk and Bulge stars (Calamida et al. 2017). The reddest (zy) LSST bands can overcome thorny problems with differential reddening (right panel in Fig. 2).

Why a deep minisurvey

- *Deep into the darkness* – The current optical photometric survey is strongly limited in the two innermost degrees above and below the Galactic plane. The absorption in these regions ranges from $A_K \sim 1$ to $A_K \sim 1.8$ mag, this means that in the visual band, A_V ranges from 10 to almost 19(!) magnitudes. However, it is significantly smaller in the redder LSST bands (see Fig. 3). Note that VVV is opening the path (Contreras Ramos et al. 2018), but the identification of variable stars is more difficult because the luminosity amplitude in the K -band is a factor of two smaller than in the iz -bands. This means that LSST can provide a complete census of RRLs even in these highly reddened regions. These new reddening maps and MDFs cover the entire Bulge and the Galactic center, thus providing the opportunity to determine the density profile of old stellar populations. Note that the Bulge and the Halo density profiles in the inner regions of the Galaxy are expected to be different: the former being steeper than the latter (Wegg & Gerhard 2013; Pérez-Villegas et al. 2017; Kunder et al. 2018; Valenti et al. 2018). There is evidence that the Bulge includes a modest fraction of dark matter (15-20%). This means a core or a mild cusp in the density profile of the dark matter halo (Portail et al. 2017) that can be easily traced with RRLs.

- *Stellar populations beyond the Galactic center* – NIR time series data collected with 1-4m class telescopes have revealed a sizable sample of classical Cepheids located in and beyond the Galactic center (Matsunaga et al. 2011; Dékány et al. 2015; Matsunaga et al. 2018; Inno et al. 2019). This means the opportunity to investigate young (10-250 Myr) stellar tracers in a region of the Disk in which our knowledge of the radial distribution and its scale height is quite poor. More recently, Kains et al. (2018) found more than 2,500 variables in a modest FoV (VIMOS at VLT) and among them more than 100 are candidate CCs that appear to be located beyond the Galactic center. The limiting magnitudes of the deep minisurvey will allow us to trace the young population in a large fraction of the Disk.

- *Absolute age distribution* – Absolute age estimates based on the magnitude of the main sequence turn off (MSTO) are affected by uncertainties in distance and in reddening correction. The difference in magnitude between the MS knee and the MSTO is independent of these uncertainties (Bono et al. 2010b). This means absolute ages that are at least factor of two more accurate than the classical ones. We plan to trace the possible occurrence of multiple ancient star formation events using the MS knee in izy bands (23.5-24.0 mag).

Why LSST. The Bulge is one of the main reasons why the ground-based observing facilities are mainly developed in the Southern Hemisphere. The unique optical characteristics of LSST and the fact that it is the first experiment collecting deep multi-band time series data over a long time interval, will allow us to provide a complete census of the Bulge stellar content.

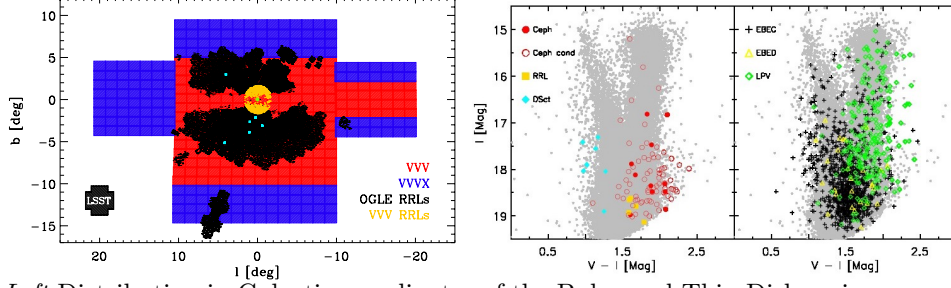


Figure 1: *Left*: Distribution in Galactic coordinates of the Bulge and Thin Disk regions covered in the NIR bands by VVV and VVVX (red and blue boxes). The black dots display the RRLs detected by OGLE IV (Pietrukowicz et al. 2015), while the yellow ones the RRLs detected by VVV (Contreras Ramos et al. 2018). The green and the magenta circles mark the Galactic center and Bulge low-reddening regions (Dutra et al. 2002). The grey area shows the FoV of LSST. *Right*: $I, V - I$ CMD of the new variables ($\sim 2,500$) identified by Kains et al. (2018).

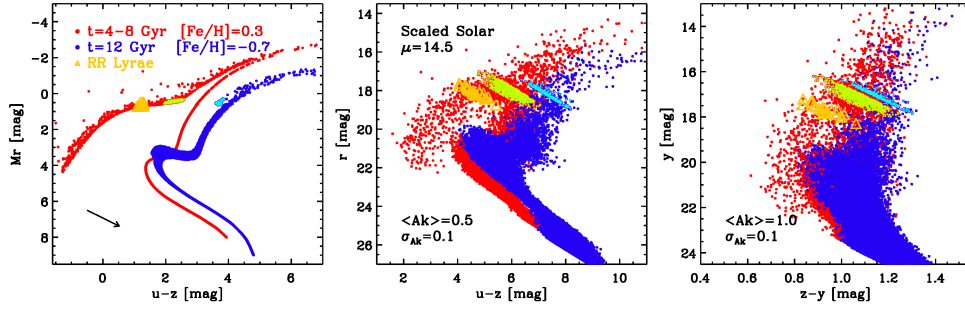


Figure 2: *Left*: $r, u - z$ synthetic CMD for two different stellar populations characterized by different metal content and chemical composition (see labeled values). The yellow triangles display RRLs, light yellow dots mark red HB stars and old RGB bump, light blue dots RC and intermediate age RGB bump. *Middle*: same as the left, but the stars were randomly perturbed by assuming a mean reddening typical of the Baade window ($A_K=0.5$ mag). *Right*: $y, z - y$ CMD, with the stars were randomly perturbed from the theoretical CMD by assuming a mean reddening of $A_K=1$ mag.

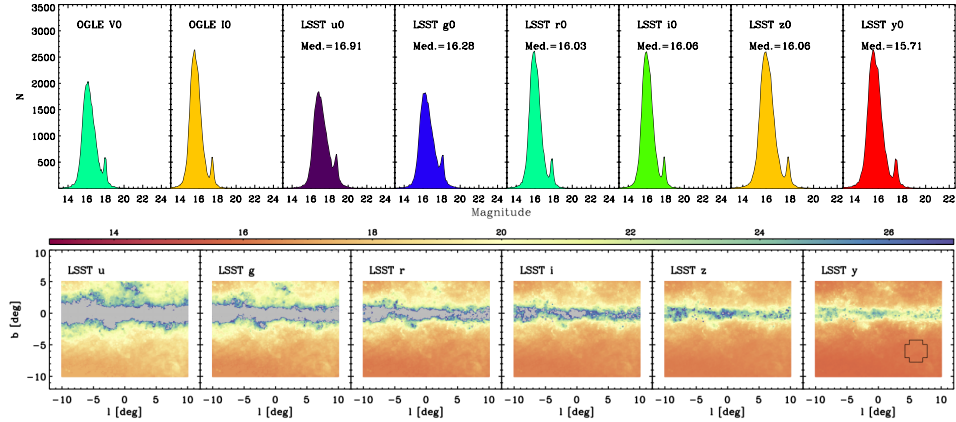


Figure 3: *Top*: From left to right, un-reddened magnitude distributions of Bulge RRLs detected by OGLEIV (V, I). They were un-reddened by using the reddening map provided by Gonzalez et al. (2012) reddening law by Cardelli et al. (1989). The expected un-reddened magnitude distributions in LSST bands (u, g, r, i, z, y) are also displayed. The V, I bands were transformed into the LSST bands by using Jordi et al. (2006) and the mean RRL colors provided by Vivas et al. (2017) and Coppola et al. (2011). *Bottom*: Apparent magnitude distribution of Bulge RRLs in Galactic coordinates for LSST bands. The color coding is plotted on top of the panels. The grey color marks areas in which the RRLs are fainter than 27 mag.

3 Technical Description

3.1 High-level description

We plan to get shallow and deep exposures with the same cadence as the WFD survey, but alternating shallow and deep exposures (see below). We will then distinguish between a shallow minisurvey and a deep minisurvey.

It is important to stress that all the subsequent discussion is based on the experience of the TVS Crowded Field Photometry Task Force (CFTF), of which one of us is the chair. The goal of the CFTF was to study the efficiency of the detection of variable stars (mainly RRLs) in very crowded fields, and to study the best data analysis strategies to find and characterize the variables. We focused on a DECam dataset (NOAO 2013A-0719, PI: A. Saha) of the Bulge, with similar characteristics (photometric depth, crowding, pixel scale) to LSST, and for which we already knew the variables from OGLE 4. The final outcome of the CFTF was that all the known bright variables, with our data analysis approach, were correctly retrieved. Furthermore, the identification of several new variables was made possible thanks to the use of a new period-search algorithm (Dall’Ora et al. 2019, in preparation).

3.2 Footprint – pointings, regions and/or constraints

- The shallow minisurvey covers an area of $-20 \lesssim l \lesssim +20$ deg and $-15 \lesssim b \lesssim +10$ deg, in all the u, g, r, i, z, y bands
- The deep minisurvey is restricted to an area of $-20 \lesssim l \lesssim +20$ deg and $-3 \lesssim b \lesssim +3$ deg and to the i, z, y bands.

3.3 Image quality

For the shallow minisurvey we can accept seeing of the order of ~ 1 arcsec. The deep minisurvey will be conducted in very highly crowded regions and, even if only the reddest bands (which provide smaller FWHMs) are requested, it is mandatory to ask for the median seeing at Cerro Pachon (~ 0.7 arcsec).

3.4 Individual image depth and/or sky brightness

- The shallow minisurvey is made of 5s+5s exposures in all the bands. This will allow us to cover the magnitude ranges shown in Tab. 1.
- The deep minisurvey will be conducted only in the i, z, y bands, aiming at identifying RRLs and RC stars in highly reddened regions of the Galactic Bulge. Indeed, according to Fig. 3, in the inner regions we expect to find the bulk of RRLs at $i, z \sim 24.5$ mag and at $y \sim 24$ mag. To reach this limits with a SNR of at least ~ 5 , we need exposure times

Table 1: Expected saturation and 5σ limits for the shallow survey.

band	saturation (mag)	5σ (mag)
u	13.5	22.2
g	14.5	23.6
r	14.6	23.1
i	14.6	22.7
z	14.1	22.1
y	12.7	21.3

of 60, 150 and 300s in the i, z, y bands, respectively. Moreover, in the less reddened (i.e. more external) regions these limits will allow us to cover the faint end of the luminosity distribution of the RRLs.

The overall proposed strategy is to collect in the internal regions (see Footprint section) the shallow + deep exposures alternatively, according to the sequence: $u, g, r, (i_{shallow}, i_{deep}), (z_{shallow}, z_{deep}), (y_{shallow}, y_{deep})$. This strategy minimizes the pointing and changing filter overheads. In the external Bulge regions we only plan to collect the shallow exposures.

These magnitudes have been computed with a custom ETC, which is based on the saturation and on the 5σ limits listed in <https://smtm-002.lsst.io/> and in <https://www.lsst.org/sites/default/files/docs/sciencebook/SB.3.pdf>.

We do not have special requirements on the sky brightness, since we ask for short exposures in the bluest bands. However, the SNR would benefit of grey time.

3.5 Co-added image depth and/or total number of visits

The final depth is not really relevant for this project, since we are interested in time-series of variable stars. However, we remark that the RC stars, which are static stars and that we use as population tracers, are already retrieved with a single visit. Finally, we note that the final stacked image will be of great interest for all the studies on the Galactic structure.

3.6 Number of visits within a night

There are no constraints on the number of visits per night, since we adopt the WFD cadence. However, since RRL light curves change significantly on short timescales, we ask a gap of at least one hour between two consecutive visits to the same pointing. Moreover, we stress again that for the internal regions we ask to collect shallow and deep exposures one after the other to save the overhead time for the change of the filter.

3.7 Distribution of visits over time

There are no particular timings or scheduling requirements. We performed a MAF analysis with the PeriodicStarFit jupyter notebook, which adopts the WFD cadence, to check the efficiency of the adopted strategy (see sect. 4).

3.8 Filter choice

For the external, less reddened regions (shallow minisurvey) we ask for the full u, g, r, i, z, y bands, since the full combination of all the filters allows us to use the REDIME technique and to disentangle the stellar populations of different metallicity. Moreover, they are also requested for the more internal regions, to study the foreground population. For the deep minisurvey, restricted to the internal regions only, we ask only for the i, z, y bands, since they are less affected by the absorption.

3.9 Exposure constraints

The 5s+5s exposures of the shallow minisurvey are designed to both avoid the saturation for the brightest RRL and RC stars, and to reach a reasonable depth at the 5σ level. Indeed, the median value of the magnitude distribution in all the bands is always reached with the total 10s exposure. The exposures of the deep minisurvey are dictated by the need to reach the RRLs in the more reddened regions. Finally, it is important to note that the deep exposures saturate at a brightness level which is well within the dynamical range of the shallow survey, being 17.9, 18.9, 19.0, 19.0, 18.5, 17.1 mag in the u, g, r, i, z, y bands, respectively.

3.10 Other constraints

The current experiment has an excellent overlap with the LSST minisurvey suggested by Gonzalez and collaborators. The reason is twofold: i) they are very much interested in tracing static stars across the Bulge and in particular in highly reddened regions. ii) they plan to complement multiband optical photometry collected with LSST with NIR photometry collected by VVV and VVVX, radial velocity measurements with multi-object spectrographs, and in particular, with new kinematical and dynamical models of the MW formation and evolution. The two groups have a significant fraction of their science in common.

The current experiment has no overlap with the minisurvey suggested by Clementini & Musella, focussed on a sample of MW dwarf satellites, since in the area we plan to cover there is only one dwarf galaxy (Sagittarius dSph). However, their observing strategy is significantly different than the current one, since they plan to use the same exposure time of the WFD survey (15/30 sec), We are suggesting shorter exposures for the shallow minisurvey and longer exposures for the deep minisurvey. Note that the current observing strategy will allow us to identify the RRLs belonging to the Sagittarius dSph and to the Sagittarius stream, since they are on average ~ 2.5 magnitude fainter than the RRLs in the Bulge. The

Sagittarius stream has already been traced in the Halo and in the Bulge, but we still lack solid constraints on the Sagittarius stream in the innermost Galactic regions.

The same applies to the Galactic plane surveys proposed by R. Street and collaborators, and by M. Lund and collaborators. They propose to increase the cadence, in order to improve the detection of variable sources for a variety of science cases. However, the quoted WPs rely on the 15/30 sec WFD observing strategy, which affects the identification and characterization of both bright and faint/reddened stellar tracers we plan to use for our science. It is worth mentioning that the standard 15/30 sec visits will allow us to trace some of the variables we are interested in, but their spatial distribution would be limited to partially reddened Bulge regions. This spotted sampling is far from being complete and homogeneous as required in a detailed survey. Note that the science drivers (REDIME) of the shallow minisurvey relies on the six u, g, r, i, z, y LSST bands.

Note that Gaia will provide a complete census of both TIICs and Miras in low reddening regions of the Galactic Bulge. These objects will be saturated in almost all the LSST bands at the distance of the Bulge, thus further supporting the complementarity between the two experiments.

Moreover, we can determine proper motions for all of our sample, either over the 10 year LSST mission, or by using existing optical and near-infrared surveys as a first epoch. Radial velocities and stellar abundances can be obtained with multi-object spectrographs such as MOONS/VLT, 4MOST/VISTA and AAOMEGA.

Finally, let us mention two independent astrophysical fields that will benefit a lot by the observing strategy and cadence we are proposing for both the shallow and the deep minisurvey.

i) *Microlensing* – The coupling between large FoV, cadence and number of visits in different photometric bands will provide unique opportunities to identify both short and long microlensing events (Navarro et al. 2018).

ii) *Galactic Supernovae* – There are reasons to believe that a significant fraction of Galactic supernovae are hidden by the Disk and the Bulge. The duration of the LSST experiment and the cadence we are suggesting will allow us to possibly identify this rare event(s).

3.11 Estimated time requirement

According to the LSST overheads, the expected total time for the internal fields (shallow + deep minisurvey) are:

- slew and setting the u filter: 120s
- 10 seconds (shallow) + 2 seconds shutter open/close: 12s
- change filter to g band: 120s
- repeat in the g band: 12s
- change filter to r band: 120s

- repeat in the r band: 12s
- change filter to i band: 120s
- 10s (shallow) + 60s (deep) + 4s shutter: 74s
- change filter to z band: 120s
- 10s (shallow) + 150s (deep) + 4s shutter: 164s
- change filter to y band: 120s
- 10s (shallow) + 300s (deep) + 4s shutter: 314s

for a time requirement per visit of 1308 seconds (21.8 minutes). Taking into account 825 visits, the total time per pointing is ~ 299.75 hours.

For the external regions we have:

- slew and setting the u filter: 120s
- 10 seconds (shallow) + 2 seconds shutter open/close: 12s
- change filter to g band: 120s
- repeat in the g band: 12s
- change filter to r band: 120s
- repeat in the r band: 12s
- change filter to i band: 120s
- repeat in the i band: 12s
- change filter to z band: 120s
- repeat in the z band: 12s
- change filter to y band: 120s
- repeat in the y band: 12s

for a time requirement per visit of 792 seconds (13.2 minutes). Taking into account 825 visits, the total time per pointing is ~ 181.5 hours.

Since the area surveyed in the internal regions is 240 square degrees (25 LSST pointings), the total time requested for the deep minisurvey is 7,494 hours.

The area surveyed in the external regions is 760 square degrees (80 LSST pointings), the total time requested for the shallow minisurvey is 14,520 hours.

In total, the time needed for both surveys would be 22,004 hours. This number has to be compared to our estimated time needed by the WFD survey to cover the same total area: 21,945 hours (912 seconds \times 825 visits \times 105 pointings).

Properties	Importance
Image quality	2
Sky brightness	2
Individual image depth	1
Co-added image depth	3
Number of exposures in a visit	1
Number of visits (in a night)	2
Total number of visits	2
Time between visits (in a night)	2
Time between visits (between nights)	2
Long-term gaps between visits	2

Table 2: **Constraint Rankings:** Summary of the relative importance of various survey strategy constraints. 1=very important, 2=somewhat important, 3=not important.

3.12 Technical trades

This is a long-term, time-series project. It will of course benefit from a good sampling of the light curves with as much as possible uniform image quality (FWHM, sky brightness). However, in our experience excellent results can be achieved even with highly non-uniform datasets [i.e. different instruments/telescopes with very different photometric depths and image quality, and non ad-hoc observing strategy, see e.g. Fiorentino et al. 2017]. Therefore, there are no really unfair trades for this project. The only constraint is the good seeing conditions for the inner regions of the Bulge, together with the proposed exposure times.

4 Performance Evaluation

The VESTALE observing strategy will allow us to secure accurate photometry (1% level) for both old ($t > 10$ Gyr) and intermediate age ($1 \lesssim t \lesssim 9$ Gyr) stellar tracers. The LSST multi-band photometry will be compared with similar Bulge data collected with DECam at 4m Blanco telescope. This means the opportunity to validate the approach adopted to perform the photometry in crowded stellar fields, and in particular, the algorithms adopted to identify and to characterize stellar variability in crowded stellar fields (see the Task Force

CFTF). Indeed, VESTALE overlaps with optical (V, I ; OGLE IV, Kains et al. 2018, see Fig. 1, right panel), NIR (Z, Y, J, H, K ; VVV, VVVX) and SDSS (u, g, r, i, z , Vivas et al. 2017) photometric time series data.

To have a quantitative reference of the expected performance, we run a MAF simulation with the PeriodicStarFit jupyter notebook, that estimates the detected fraction of the input variable stars. By putting the RRLs expected reddened median (with respect to the total distribution) magnitudes, according to the simulation we can correctly retrieve $\sim 40\%$ of the periods after only one year (see Fig. 4). We stress that the plot shows the fraction of the detected variables at the median magnitude level, which is 19.9, 18.6, 18.2, 17.8, 17.4, 16.8 mag in the u, g, r, i, z, y bands, respectively. This means that the efficiency is higher at brighter magnitudes. Indeed, it is almost 100% after one year for the bright end of the magnitude distribution. Fig. 5 and Fig. 6 show the same analysis, but for the TIICs and the CCs. All the simulations are based on the known sample of variables, released by OGLE IV. In particular, we want to stress that the simulation on CCs is depicting the worst case (low period, small amplitude variables), and has to be considered as an "acid test". It is worth mentioning that, after the first observing season, we are going to get efficiencies comparable to those of Gaia and of the currently available Galactic plane surveys.

As a technical comment, we stress that we could not change the (15 + 15) sec WFD visit in our simulations, and we simply scaled, in the PeriodicStarFit jupyter notebook, the reference magnitudes by the differences in the expected flux ratios on the basis of our exposure times. Moreover, we ran our simulation over the entire WFD area. Our analysis could be improved with an *ad-hoc* simulation on the actual area and with the actual exposure times. The PeriodicStarFit notebook is available in the standard `maf_local/sims_maf_contrib/science/periodicVariables` directory. It is based on the `/home/docmaf/maf_local/sims_maf_contrib/mafContrib/periodicStarMetric.py` code.

5 Special Data Processing

There are no special data processing requirements, since we adopt the same visit strategy as the WFD survey, with different exposure times.

6 Acknowledgement

This work was developed within the Transient and Variable Stars Science Collaboration (TVS) and the authors acknowledge the support of TVS in the preparation of this paper.

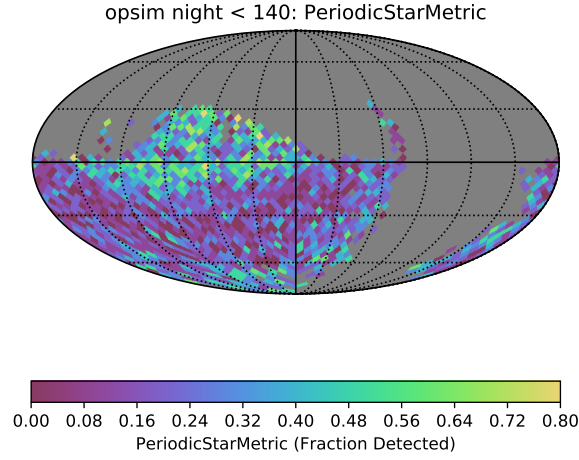


Figure 4: Fraction of RR Lyrae stars detected after one year. For the simulation, we adopted an average period of 0.6d and an average amplitude of 0.5 mag at the expected median level of the RRLs magnitudes distribution. The map is based on the baseline2018a simulation, and it includes all the sky covered by the WFD survey. However, only the central part of the map is relevant for our project.

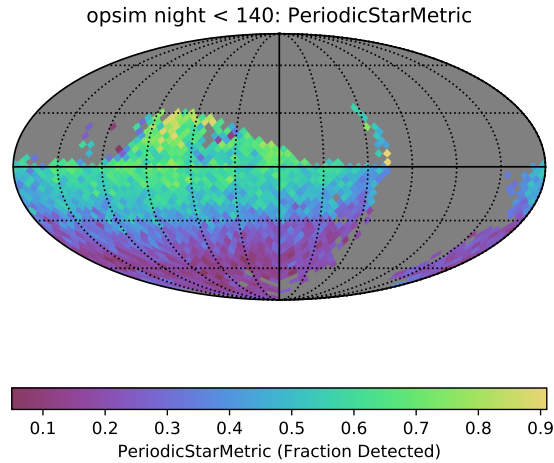


Figure 5: Fraction of Type II Cepheids stars detected after one year. For the simulation, we adopted an average period of 2.0d and an average amplitude of 0.6 mag and at the expected median level of the TIICs magnitudes distribution. The map is based on the baseline2018a simulation, and it includes all the sky covered by the WFD survey. However, only the central part of the map is relevant for our project.

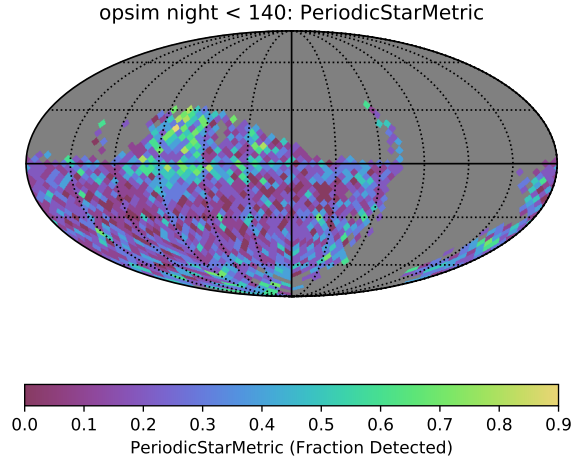


Figure 6: Fraction of Classical Cepheids detected after one year. For the simulation, we adopted a period of 1.0d, corresponding to the mode of the CCs periods distribution, and an amplitude of 0.15 mag (corresponding to the typical amplitude of the 1.0d CCs) and at the expected median level of the 1.0d CCs magnitudes distribution. The map is based on the baseline2018a simulation, and it includes all the sky covered by the WFD survey. However, only the central part of the map is relevant for our project. Note also that in this simulation we studied the worst case, i.e. low period and small amplitudes CCs.

7 References

- Athanassoula, E. 2005, *MNRAS*, 358, 1477
- Barbuy, B., Chiappini, C., & Gerhard, O. 2018, *ARA&A*, 56, 223
- Bono, G., Iannicola, G., Braga, V. F., et al. 2018, *ApJ*, accepted, arXiv181107069B
- Bono, G., Stetson, P. B., Walker, A. R., et al. 2010a, *PASP*, 122, 651
- Bono, G., Stetson, P. B., VandenBerg, D. A., et al. 2010b, *ApJL*, 708, L74
- Bono, G., Genovali, K., Lemasle, B., et al. 2015, in *ASPCS*, Vol. 491, *Fifty Years of Wide Field Studies in the Southern Hemisphere: Resolved Stellar Populations of the Galactic Bulge and Magellanic Clouds*, ed. S. Points & A. Kunder, 148
- Calamida, A., Strampelli, G., Rest, A., et al. 2017, *AJ*, 153, 175
- Cardelli, J. A., Clayton, G. C., & Mathis, J. S. 1989, *ApJ*, 345, 245
- Carollo, D., Beers, T. C., Lee, Y. S., et al. 2007, *Nature*, 450, 1020
- Catchpole, R. M., Whitelock, P. A., Feast, M. W., et al. 2016, *MNRAS*, 455, 2216
- Contreras Ramos, R., Minniti, D., Gran, F., et al. 2018, *ApJ*, 863, 79
- Coppola, G., Dall’Ora, M., Ripepi, V., et al. 2011, *MNRAS*, 416, 1056
- Dékány, I., Minniti, D., Catelan, M., et al. 2013, *ApJL*, 776, L19
- Dékány, I., Minniti, D., Majaess, D., et al. 2015, *ApJL*, 812, L29
- Dutra, C. M., Santiago, B. X., & Bica, E. 2002, *A&A*, 381, 219
- Fabrizio, M., Bono, G., Nonino, M., et al. 2016, *ApJ*, 830, 126
- Fiorentino, G., Bono, G., Monelli, M., et al. 2015, *ApJL*, 798, L12
- Fiorentino, G., Monelli, M., Stetson, P. B., et al. 2017, *A&A*, 599, A125
- Freeman, K., Ness, M., Wylie-de-Boer, E., et al. 2013, *MNRAS*, 428, 3660

Gonzalez, O. A., Rejkuba, M., Zoccali, M., et al. 2012, *A&A*, 543, A13
Hammersley, P. L., Garzón, F., Mahoney, T. J., López-Corredoira, M., & Torres, M. A. P. 2000, *MNRAS*, 317, L45
Hill, V., Lecureur, A., Gómez, A., et al. 2011, *A&A*, 534, A80
Inno, L., Urbaneja, M. A., Matsunaga, N., et al. 2019, *MNRAS*, 482, 83
Jordi, K., Grebel, E. K., & Ammon, K. 2006, *A&A*, 460, 339
Kains, N., Calamida, A., Rejkuba, M., et al. 2018, *MNRAS*, arXiv:1805.01898
Kinman, T. D., Cacciari, C., Bragaglia, A., Smart, R., & Spagna, A. 2012, *MNRAS*, 422, 2116
Kunder, A., & Chaboyer, B. 2008, *AJ*, 136, 2441
Kunder, A., Rich, R. M., Koch, A., et al. 2016, *ApJL*, 821, L25
Kunder, A., Valenti, E., Dall’Ora, M., et al. 2018, *SSRv*, 214, 90
Matsunaga, N., Bono, G., Chen, X., et al. 2018, *SSRv*, 214, 74
Matsunaga, N., Kawadu, T., Nishiyama, S., et al. 2011, *Nature*, 477, 188
Matsunaga, N., Feast, M. W., Bono, G., et al. 2016, *MNRAS*, 462, 414
McCarthy, I. G., Font, A. S., Crain, R. A., et al. 2012, *MNRAS*, 420, 2245
Monelli, M., Milone, A. P., Fabrizio, M., et al. 2014, *ApJ*, 796, 90
Navarro, M. G., Minniti, D., Contreras-Ramos, R., 2018, *ApJ*, 865, 5
Ness, M., Freeman, K., Athanassoula, E., et al. 2012, *ApJ*, 756, 22
Pérez-Villegas, A., Portail, M., & Gerhard, O. 2017, *MNRAS*, 464, L80
Pietrukowicz, P., Kozłowski, S., Skowron, J., et al. 2015, *ApJ*, 811, 113
Rojas-Arriagada, A., Recio-Blanco, A., Hill, V., et al. 2014, *A&A*, 569, A103
Salaris, M., Percival, S., & Girardi, L. 2003, *MNRAS*, 345, 1030
Schönrich, R., Asplund, M., & Casagrande, L. 2014, *ApJ*, 786, 7
Shen, J., Rich, R. M., Kormendy, J., et al. 2010, *ApJL*, 720, L72
Stetson, P. B., Monelli, M., Fabrizio, M., et al. 2011, *The Messenger*, 144, 32
Valenti, E., Zoccali, M., Gonzalez, O. A., et al. 2016, *A&A*, 587, L6
Valenti, E., Zoccali, M., Mucciarelli, A., et al. 2018, *A&A*, 616, A83
Vivas, A. K., Saha, A., Olsen, K., et al. 2017, *AJ*, 154, 85
Wegg, C., & Gerhard, O. 2013, *MNRAS*, 435, 1874
Zoccali, M., Valenti, E., & Gonzalez, O. A. 2018, *A&A*, 618, A147
Zoccali, M., Gonzalez, O. A., Vasquez, S., et al. 2014, *A&A*, 562, A66
Zoccali, M., Vasquez, S., Gonzalez, O. A., et al. 2017, *A&A*, 599, A12